Purdue University
Purdue e-Pubs

International Refrigeration and Air Conditioning Conference | School of Mechanical Engineering

2014

Shape Optimization of a Compressor Supporting Plate Based on Vibration Modes

Olavo M. Silva
Federal University of Santa Catarina, Brazil, olavo@lva.ufsc.br

Thiago M. Guesser
Federal University of Santa Catarina, Brazil, thiagomannes@hotmail.com

Igor M. Guesser
Federal University of Santa Catarina, Brazil, igorguesser@hotmail.com

Claudio de Pellegrini
EMBRACO, Research & Development Group, Brazil, claudio.pellegrini@embraco.com

Carlos E. Vendrami
EMBRACO, Research & Development Group, Brazil, carlos_vendrami@embraco.com.br

See next page for additional authors

Authors
Olavo M. Silva, Thiago M. Guesser, Igor M. Guesser, Claudio de Pellegrini, Carlos E. Vendrami, and Arcanjo Lenzi

Shape Optimization of a Compressor Supporting Plate Based on Vibration Modes

Olavo M. SILVA[1]*, Thiago M. GUESSER[1], Igor M. GUESSER[1], Claudio de PELLEGRINI[2], Carlos E. VENDRAMI[2], Arcanjo LENZI[1]

[1]Mechanical Engineering Department, Federal University of Santa Catarina,
Florianopolis, SC, Brazil
olavo@lva.ufsc.br

[2]EMBRACO, Research & Development Group,
Joinville, SC, Brazil
claudio.pellegrini@embraco.com

* Corresponding Author

ABSTRACT

In typical household refrigeration systems, the compressor is structurally connected to the cabinet through an assembly composed of rubber mounts and a steel support plate, usually called base-plate. This plate works as a vibration energy path from the compressor to other refrigerator components, and its dynamic behavior must be known in order to avoid the coincidence of resonances and operational frequencies , a situation in which the energy flow is maximized. One way to design a support that satisfies this requirement is to optimize the shape of the plate, locating its structural modes as far as possible from the operational frequency and first harmonics. In this work, the Finite Element Method (FEM) is used to solve the eigenvalue problem and to parameterize the optimization procedure, which is based on positioning of the nodes of a design region (the plate) in a FEM simplified model. Due to the large number of variables, a gradient-based method is adopted. The objective of the methodology is to maximize the difference between two adjacent eigenvalues near the fundamental operation frequency of the compressor, in order to obtain a large and effective bandgap. A geometrical constraint is imposed to the problem and it is represented by a maximum allowed deformation of the plate. The gradients needed are obtained using elementary stiffness and mass matrices information. The obtained results show that the procedure leads to a new shape which ensures the desired dynamic characteristics for the support plate.

1. INTRODUCTION

Experimental results from several academic and industrial researches have shown that compressor and fan are the main noise sources in a domestic refrigeration system. Simpler refrigerators do not use fan, while high-end refrigerators commonly use fans with low noise and vibration levels. Thus, generally, the compressor is considered the major source of energy for most cases when dealing with noise in refrigerators. Transient excitations generated by the compression process are considered quasi-periodic signals, with fundamental frequency equals to the compressor operation frequency (60Hz in North America and Latin America and 50Hz in Europe and Asia). In practice, as the signals are quasi-periodic, several harmonics are present in the spectrum representation. Another important source of vibration is the compressor unbalance, which generates high vibration levels mainly in the fundamental frequency and first harmonics. Therefore, it is assumed in this work that the characteristic excitation of a compressor has the spectral distribution schematically illustrated in Figure 1.

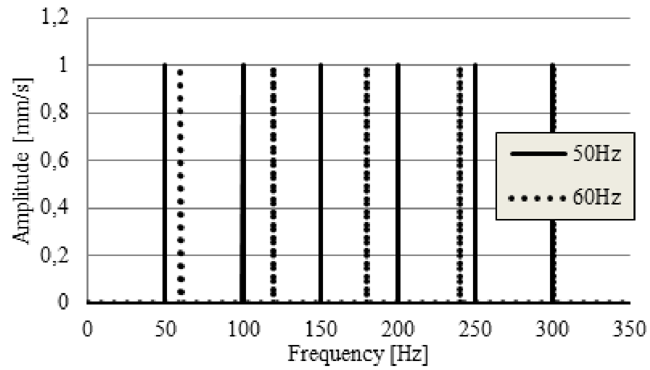

Figure 1: Characteristic spectrum of compressor excitations.

The support base-plate of a refrigerator is responsible for the structural connection between the cabinet and the compressor, which is its primary function. However, the plate must attend some requirements, among them, to have low dynamic response during operation of the compressor. The correct dynamic response of the plate is important for filtering the vibrations of the compressor, reducing the energy transmitted to the cabinet, as well as for not allowing excessive noise radiation. The project of a base-plate with desirable vibration characteristics consists on allocating its structural modes as far as possible from the operational frequency and first harmonics. This work presents a design methodology for this structure by the use of an optimization procedure. In Section 2, the vibration problem is defined, as well as the optimization problem and its peculiarities. In this article, a gradient-based method is used to solve the optimization problem. Section 3 describes the necessary gradients of the considered functions. In Section 4, some numerical issues are presented and, finally, Section 5 and 6 present the results and conclusions of this work.

2. PROBLEM DEFINITION

2.1 Simplified Finite Element Model

The differential equation which describes the motion of a body is solved by FEM, by discretizing its geometrical domain, yielding to a representation by several elements. Thus, an undamped free vibration problem can be represented as

$$(\boldsymbol{K} - \lambda_i \boldsymbol{M})\boldsymbol{\Phi}_i = 0 \quad (1)$$

where $\boldsymbol{K}$ and $\boldsymbol{M}$ are the global stiffness and mass matrices, respectively; λ_i is the i-th eigenvalue, and $\boldsymbol{\Phi}_i$ is its respective eigenvector. The finite element formulation to be used must be chosen correctly, based on the geometry of the structure and on the degrees of freedom to be considered in the problem. In this work, the optimization procedure requires a good representation of the base-plate, so that an Experimental Modal Analysis is performed to assist on the choice of best element formulation. The methodology presented here starts with a steel flat plate, with 570x135mm, and 2mm thick. The experimental set up can be seen in Figure 2. The objective of this test is to compare different types of elements, verifying the differences between experimental and numerical results in a free configuration. In order to perform the numerical modal analysis, the commercial software ANSYS® 12.1 is used in this work. The following elements were tested:

- quadrangular shell with linear shape functions (SHELL181);
- quadrangular shell with quadratic shape functions (SHELL281);
- hexahedral solid with linear shape functions (SOLID45);
- hexahedral solid with quadratic shape functions (SOLID95);
- hexahedral solid with linear shape functions and non-conforming formulation (SOLID45 + KEYOPT(1)=0 "*Include extra displacement shapes*").

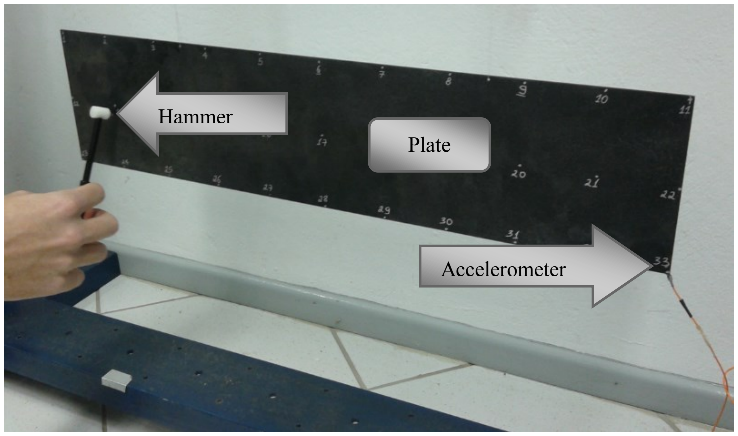

Figure 2: Experimental Modal Analysis of a free flat plate.

The last one in the list above is a linear solid element with temporary addition of 3 extra shape functions, with maximum value defined at the geometric center of the element. The related formulation is described in Zienkiewcz *et al.* (2005). This element type has a good representation of shear effects due to the extra shape functions considered on the stiffness matrices calculation. The element size used for all tested models is sufficiently small to represent the dynamic behavior of the plate up to the maximum frequency considered (500Hz). A regular mesh is used, with only one element on the thickness. A comparison between numerical and experimental natural frequencies is presented in Table 1.

Table 1: Natural modes of the studied plate.

Natural frequency order	Measured	SHELL181	SHELL281	SOLID45	SOLID95	SOLID45 non-conforming
1	**34,1**	34,1	34,1	56,5	34,1	34,1
2	**88,7**	87,4	87,2	88,6	87,3	87,4
3	**94,3**	94,5	94,5	155,9	94,5	94,5
4	**182,8**	180,6	180,2	190,4	180,4	180,7
5	**185,6**	186,3	186,1	306,0	186,2	186,3
6	**288,1**	285,1	284,4	317,2	284,7	285,2
7	**307,6**	309,2	308,8	479,4	308,9	309,3
8	**407,8**	405,6	404,6	506,4	405,1	405,9
9	**460,0**	462,7	461,9	684,3	462,0	462,8
10	**547,3**	546,6	545,2	756,5	545,8	547,0

Such discrepancy in the results of linear solid element (SOLID45) is due to the poor representation of bending in its formulation. In other hand, the non-conforming version of linear element (SOLID45 non-conforming) presents results which agree with shell and quadratic elements. Thus, by having simple implementation and good results, this last formulation is chosen in this work. The use of an element type with simpler formulation facilitates the analytical calculation of gradients, which will be described in Section 3. Shell elements, although simpler to apply, have greater difficulties in numerical implementation, particularly in three-dimensional cases.

After choosing the proper element to be used, a FE model of the assembly composed by base-plate and compressor was developed. The plate was considered clamped at both lateral ends, and the compressor was considered as a concentrated mass rigidly connected to the plate. Here, only the inertial effects of the compressor are taken into account, and the elastic effects of the rubber mounts were neglected. Compressor dimensions, total mass (8.5kg) and spatial position were obtained from the catalogue of the product. Figure 3 shows the mesh of the FE model.

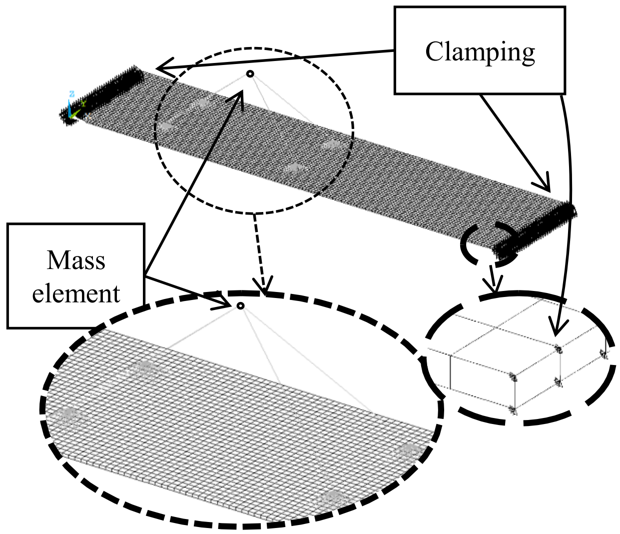

Figure 3: Simplified FE model.

Rigid beam elements with negligible mass were used to connect the mass element to the plate, through 4 regions with area equivalent to the mounts size. Besides the total mass, the moments of inertia of the compressor were considered in the properties of the mass element. The first modes of this simplified structure can be seen in Figure 4.

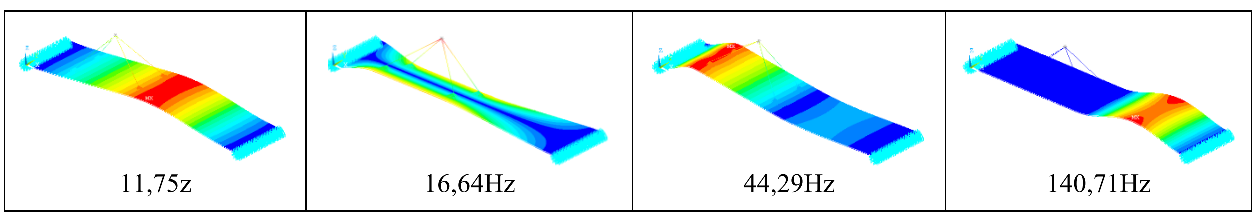

Figure 4: First modes of the simplified FE model.

2.2 Parameterization of the problem

This work proposes the use of Cartesian coordinates of the nodes which composes the base-plate FE mesh as design variables of an optimization procedure. However, only changes on the perpendicular direction is allowed (Z-direction). In order to keep the thickness of the plate constant (2mm), and remembering that just one element is used to discretize this dimension, the movement of a top node is constrained to the movement of its respective bottom node, as can be seen in Figure 5. So, each design variable of the problem is associated with the movement of a pair of nodes, called in this work as “twin nodes”. Thus, the optimization algorithm interprets only the Z-coordinates of the nodes related to the bottom of the plate, since the position of other nodes is mathematically linked as

$$z_j = \begin{cases} z_j, & for\ \ j = 1,2,3,4 \\ z_{j-4} + thk, & for\ j = 5,6,7,8 \end{cases}, \qquad (2)$$

where thk is the thickness of the plate, and the connectivity diagram is shown in Figure 5.

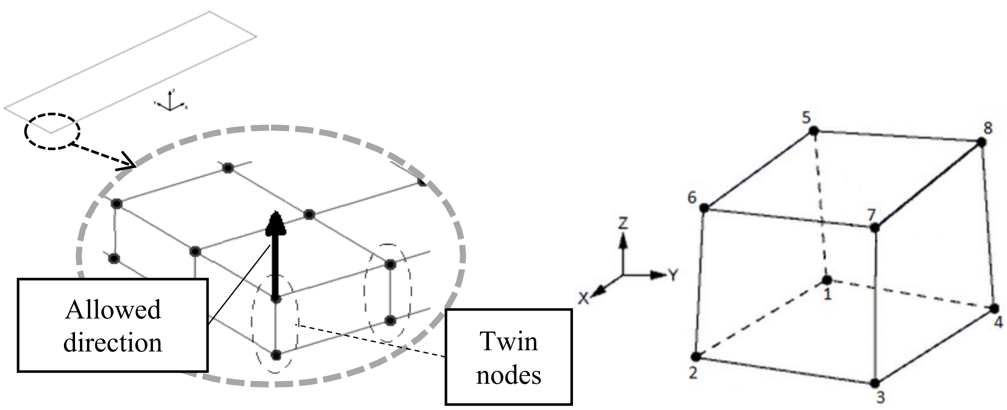

(a) **(b)**

Figure 5: (a) Parameterization. (b) Standard solid finite element.

For each optimization step, a new set of design variables (vector $\boldsymbol{z}$ containing the Z-coordinates of the nodes related to the bottom of the plate) is obtained, enabling the actualization of the FE mesh based on the z_j coordinate and on the thickness thk.

2.3 Optimization Problem

The objective of this work is to enforce a band-gap in the base-plate vibration spectrum around the fundamental frequency of excitation (here, 50Hz). For this purpose, an optimization procedure is applied to vary the natural frequencies of this plate, based on the parameterization described in Section 2.2. Observing Table 2, one can note that the value of the 3rd natural frequency of the system is 44,3Hz, very close to the fundamental frequency of excitation. The authors suggest tuning this structural mode to 75Hz, avoiding the resonances near 50Hz. Consequently, due to the target value of this tuning, the 3rd mode will be also far from 100Hz, the first excitation harmonic.
A general optimization problem can be defined as:

$$\begin{array}{c} \min f(\boldsymbol{z}) \\ subject\ to\ g(\boldsymbol{z}) \leq 0 \ , \\ z_{low} \leq z_i \leq z_{upper} \end{array} \quad (3)$$

where $f(\boldsymbol{z})$ is the objective function, $g(\boldsymbol{z})$ is the constraint function, generally related to a physical or manufacturing requisite, and $\boldsymbol{z}$ is the vector of design variables, which are bounded by z_{low} and z_{upper}. In this work,

$$f(\boldsymbol{z}) = (\lambda_3 - 2\pi 75)^2, \quad (4)$$

where λ_3 is the 3rd eigenvalue of the system.
Since the modification of twin nodes coordinates are enabled only for Z-direction and considering the plate thickness constant, elementary volumes do not change along the process. So, a mass constraint, widely used in optimization procedures, cannot be used. Therefore, this work proposes a measure of mesh distortion as a constraint for the optimization problem, defined as

$$g(\boldsymbol{z}) = \frac{1}{N_e} \sum_{e=1}^{N_e} \overline{L_e}, \quad (5)$$

where N_e is the number of finite elements in the plate, and $\overline{L_e}$ is the average edge of each element bottom's face, defined as

$$\overline{L_e} = \frac{|n_2 - n_1| + |n_3 - n_2| + |n_4 - n_3| + |n_1 - n_4|}{4}. \quad (6)$$

with n_1, n_2, n_3 and n_4 being the coordinates of the bottom nodes of element e (see Figure 5b). The symbol | | is associated with the norm of the distance between two nodes.

3. SENSITIVITY ANALYSIS

As a gradient-based optimization method will be used in this work, derivatives of the objective function and constraints are needed. Using symmetry properties of mass and stiffness matrices, the derivative of the i-th eigenvalue of a system related to the j-th component of design variable vector $\boldsymbol{z}$ can be obtained by (Haftka and Gurdal, 1992)

$$\frac{\partial \lambda_i}{\partial z_j} = \boldsymbol{\Phi}_i^{\mathrm{T}} \left(\frac{\partial \boldsymbol{K}}{\partial z_j} - \lambda_i \frac{\partial \boldsymbol{M}}{\partial z_j} \right) \boldsymbol{\Phi}_i, \quad (7)$$

considering the eigenvectors normalized by the mass matrix. By this way, the sensitivity of a eigenvalue related to a perturbation z_j on Z-coordinate depends on the respective derivatives of mass and stiffness matrix. When a node has its coordinates changed, only the elements in the vicinity are distorted. Thus, one can prove that Equation 7 can be rewritten as

$$\frac{\partial \lambda_i}{\partial z_j} = \sum_{e=1}^{N_v} \left(\boldsymbol{\Phi}_{ie}^{\mathrm{T}} \left(\frac{\partial \boldsymbol{K}_e}{\partial z_j} - \lambda_i \frac{\partial \boldsymbol{M}_e}{\partial z_j} \right) \boldsymbol{\Phi}_{ie} \right), \quad (8)$$

where N_v is the number of elements in which node j takes part; $\boldsymbol{\Phi}_{ie}$ is the vector corresponding to the entries of eigenvector $\boldsymbol{\Phi}_i$ related to the element e degrees of freedom; and $\boldsymbol{K}_e$ and $\boldsymbol{M}_e$ are, respectively, the elementary stiffness and mass matrices related to element e.

One can observe, from Equation 8, that the extra calculation required are the derivatives of elementary matrices, since the eigenvector and eigenvalue are directly obtained by modal analysis in the current iteration. As seen previously, the proposed parameterization do not change the volume of each element. So, $\partial \boldsymbol{M_e} / \partial z_j = 0$ for all elements of the plate. Calculation of elementary stiffness derivatives is based on FE procedure, and can be obtained as follows:

$$\frac{\partial \boldsymbol{K}_e}{\partial z_j} = \sum_{p=1}^{N_p} \left(\frac{\partial \boldsymbol{B}_e}{\partial z_j}^{\mathrm{T}} \boldsymbol{C} \boldsymbol{B}_e(p) \det(\boldsymbol{J}_e) + \boldsymbol{B}_e{}^{\mathrm{T}} \boldsymbol{C} \frac{\partial \boldsymbol{B}_e(p)}{\partial z_j} \det(\boldsymbol{J}_e) + \boldsymbol{B}_e(p)^{\mathrm{T}} \boldsymbol{C} \boldsymbol{B}_e(p) \frac{\det(\boldsymbol{J}_e)}{\partial z_j} \right) \alpha_p, \quad (9)$$

where $\boldsymbol{C}$ is the constitutive matrix, $\boldsymbol{B}_e$ is the matrix of shape functions derivatives in element local coordinates, and $\boldsymbol{J}_e$ is the *Jacobian* matrix (Bathe, 1996). Equation 9 refers to a numeric integration, with N_p integration points (p) obtained from the Gauss rule. The weight factor α_p is related to the chosen integration points. All analytical developments for finding the derivatives of elementary stiffness matrices, based on Equation 9, is purposely omitted of this article. As mentioned above, solid elements with non-conforming formulation will be used on the modeling of the plate, and its FE equations must be considered.

Now, using Equation 8 and 9, the derivatives of Equation 4 can be obtained by

$$\frac{\partial f(\boldsymbol{z})}{\partial z_j} = 2(\lambda_3 - 2\pi 75) \frac{\partial \lambda_3}{\partial z_j}. \quad (10)$$

On the other hand, the derivatives of constraint function (Equation 5) are directly calculated by

$$\frac{\partial g(\boldsymbol{z})}{\partial z_j} = \frac{1}{N_e} \sum_{e=1}^{N_e} \frac{\partial \overline{L_e}}{\partial z_j}. \quad (11)$$

For example, for a node j referent to position 1 in Figure 5b in an element e, one can obtain

$$\frac{\partial \overline{L_e}}{\partial z_j} = \frac{1}{4} \left(\frac{1}{|n_2 - n_j|} (z_2 - z_j) + \frac{1}{|n_j - n_4|} (z_j - z_4) \right). \quad (12)$$

4. NUMERICAL PROCEDURE

4.1 Gradient-based algorithm

The optimization procedure proposed was implemented with a MATLAB® version of the Method of Moving Asymptotes (MMA), developed by Svanberg (1987). A simple program interface was written for reading and writing the relevant data from files used in both FEM software and MMA optimizer, and to calculate numerically the objective and constraint function sensitivities. It was defined an iterative procedure following the steps: i) input initial design values; ii) enter the optimization loop. It calls the FEM program (after writing the current iteration values of design variables to a file) to run a modal analysis in batch mode and return to optimization procedure the eigenvalues and eigenvectors; iii) calculate the sensitivities in the interface module and send these information to MMA; iv) if attended the stopping criteria, stop the optimization and plot the optimized design. Otherwise, repeat from (ii).

4.2 Initial design

A design point referent to a totally flat plate infers to numerical instabilities in the sensitivities calculation (Leiva, 2003). This problem occurs due to the symmetry of the geometry in Z-direction, since a node movement in negative or positive sense leads to the same values on derivatives of the objective function. In order to overcome this problem, it is suggested a slight initial deformation of the plate proportional to the shape of the mode to be optimized (values lower than 1mm). This problem can be better understood by observing the distribution of the sensitivities over the plate in Figure 6. Note that, for a flat initial design, there is not a defined pattern on the distribution of the sensitivities, while using a slight initial perturbation the results obtained are more comprehensive. For the sake of simplicity, this test is performed in the absence of the compressor in the model.

Initial design: flat plate	
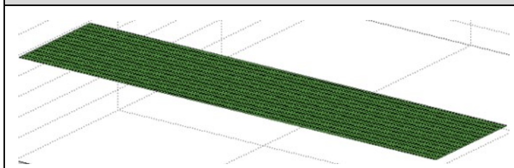	Zero initial deformation
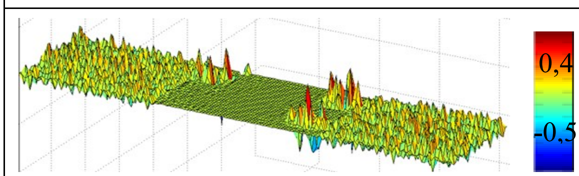	Calculated derivatives of objective function

(a)

Initial design: proportional to a mode shape	
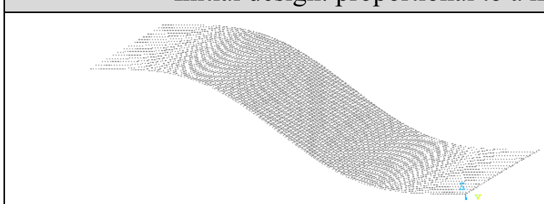	Slight initial deformation based on a mode shape (graphically amplified)
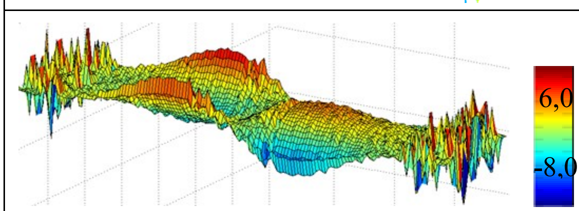	Calculated derivatives of objective function

(b)

Figure 6: Sensitivities distribution.

However, it can be seen some instabilities in regions near boundary conditions, probably caused by numerical truncation on very low derivative values. This problem, which can disturb the optimization process, is solved by applying a sensitivity filter.

4.3 Sensitivity filter

In order to avoid abrupt variation on the objective function derivatives along the design domain, this work suggests the use of a methodology presented by Bendsøe and Sigmund (2003), in which a filter is applied to obtain a weighted local average of the derivative values. Here, this filter is adapted and defined as

$$\overline{\frac{\partial f(\boldsymbol{z})}{\partial z_j}} = \frac{1}{\sum_{i=1}^{N_{filt}} H_i} \sum_{i=1}^{N_{filt}} H_i \frac{\partial f(\boldsymbol{z})}{\partial z_j}. \tag{13}$$

where N_{filt} is the number of i nodes inside a defined search radius r_{min} , and $H_i = r_{min} - distance(j,i)$. After numerical tests, this filter is used in this work with $r_{min} = 10mm$. This procedure is performed to each design variable (node position), for all iterations, based on a matrix obtained in the beginning of the whole process (with all nodes and its neighborhood).

The same sensitivity distribution shown in Figure 6b, without filter, is presented in Figure 7, with application of Equation 13 using $r_{min} = 10mm$. All major instabilities were removed with this procedure.

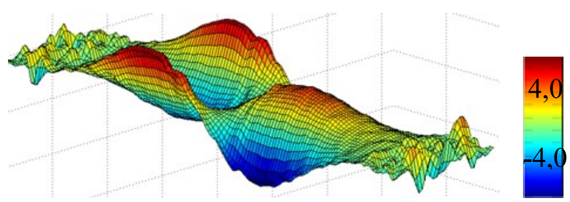

Figure 7: Filtered sensitivities distribution.

5. RESULTS

The procedure described in the sections above is applied for the simplified model presented in Figure 4. After numerical tests, the value chosen for the constraint limit is 100,1% of its initial value, in order to prevent a large distortion of the plate. The bounds for the design variables are defined as $z_{lower} = -10mm$ and $z_{upper} = 10mm$. Furthermore, a sensitivity filter with $r_{min} = 10mm$ is applied. The 3th mode is used to create the initial deformation. The variation of the first five natural frequencies along the optimization procedure can be seen in Figure 8.

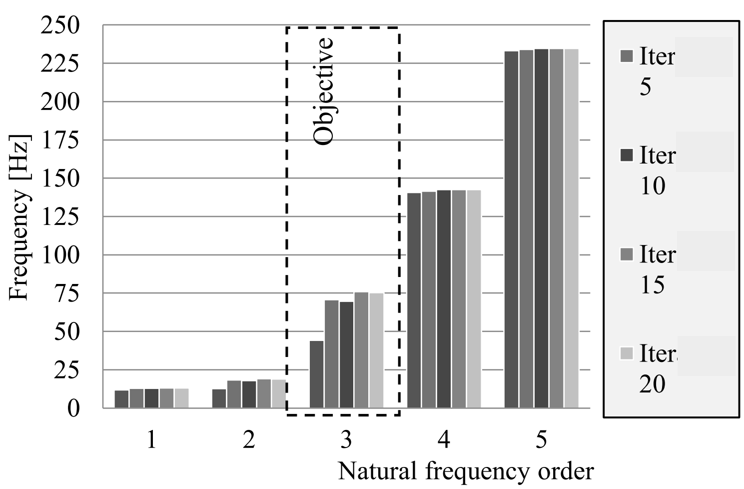

Figure 8: Natural frequencies of the model along the optimization procedure.

After 20 iterations, the optimization procedures reaches the objective of tuning the 3th mode to 75Hz, without violation of the constraint function. An interesting observation to be pointed is that there are no significant changes in the values of others eigenvalues. The final shape with an amplified scale can be seen in Figure 9, while the mesh with real deformation is presented in Figure 10. One can see that a little variation on the shape of the base-plate is sufficient to rearrange its initial modes.

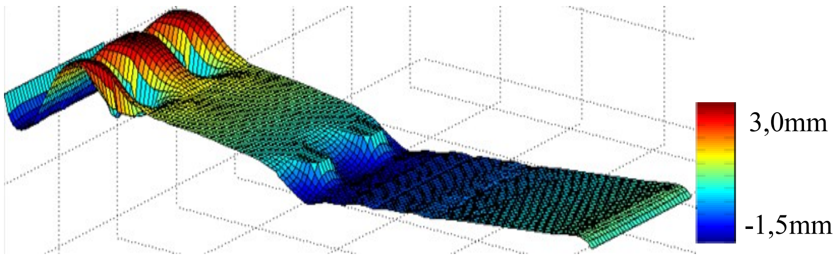

Figure 9: Final design of the base-plate (amplified scale).

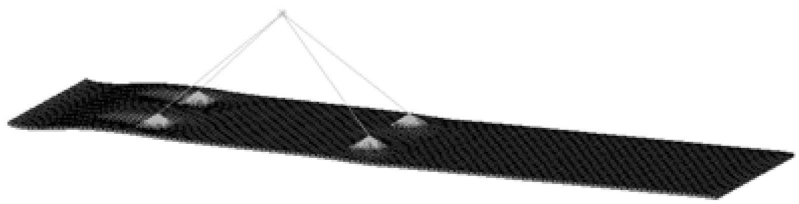

Figure 10: Final design of the base-plate.

In this work, the same mode used in tuning was used as a profile to the initial deformation. However, other modes could be used, leading to possibly different final designs (this problem has, probably, multiple local minima). Finally, to verify the quality of solid finite element mesh of the resulting design, the same case was performed with shell elements, indicating no significant differences on the values of natural frequencies.
Sound Power Level of vibrating structures are directly related to its spatial mean square velocity (Fahy, 2001). This measure, for an unitary force applied on mass element, is obtained by harmonic analysis with damping factor 0,03%, and it is graphically presented in Figure 11. A good behavior for 50 and 100Hz can be observed.

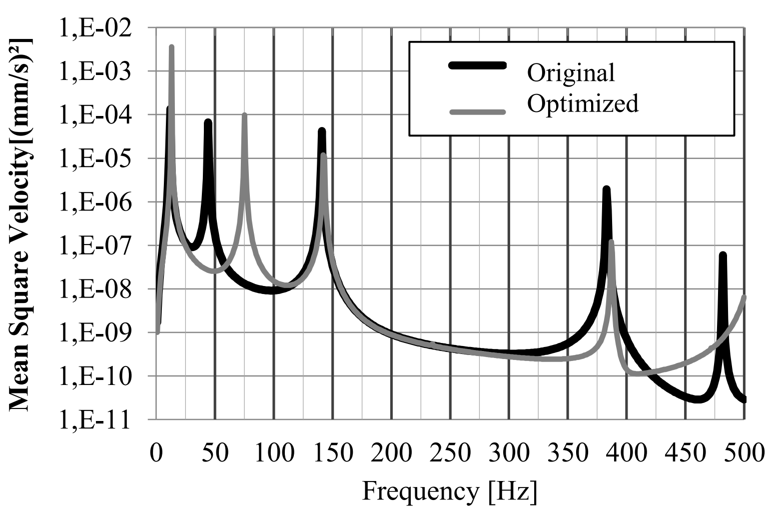

Figure 11: Mean square velocity of the plate: original vs. optimized.

6. CONCLUSIONS

Structural shape optimization has proven to be an excellent tool in design of new components. The great advantage of methods based on the movement of nodes is the possibility of creating unconventional geometries, hardly obtained by traditional parametric methods. The application of this method, however, is not a simple task, and varies depending on the problem studied. In this work, the dynamic behavior of a support base-plate was changed by tuning the 3rd mode of the structure, in order to guarantee that the fundamental frequency and the first harmonic of excitation do not cause excessive vibration on the system. The obtained results show that the procedure leads to a new shape that ensures the desired dynamic characteristics for the support plate. A more realistic model can be used for more accurate results, and an experimental validation is recommended.

NOMENCLATURE

FE	finite element
$\boldsymbol{K}$	stiffness matrix
$\boldsymbol{M}$	mass matrix
$\boldsymbol{\Phi}$	eigenvector
λ	eigenvalue
z	perturbation on Z-direction
thk	thickness
L	element edge
n	node position
$\boldsymbol{C}$	constitutive matrix
$\boldsymbol{B}$	matrix of shape functions derivatives
$\boldsymbol{J}$	Jacobian
MMA	Method of Moving Asymptotes
r_{min}	filter radius

REFERENCES

Bathe, K., 1996, *Finite Element Procedures*, Prentice-Hall Inc., New Jersey.

Bendsøe, M. P, Sigmund, O., 2003, *Topology Optimization: Theory, Methods and Applications*, 2nd Edition, Springer, Berlin.

Fahy, F., 2001, *Engineering Acoustics*, Academic Press, London.

Haftka, R. T., Gurdal, Z., 1992, *Elements of Structural Optimization*, 3rd edition, Kluwer Academic Publishers, Netherlands.

Leiva, J. P., 2003, Method For Generating Perturbation Vectors For Topography Optimization of Structures, *5th World Congress of Structural and Multidisciplinary Optimization*, Venice.

Svanberg, K., 1987, The method of moving asymptotes - a new method for structural optimization, *International Journal for Numerical Methods in Engineering*, vol.24, p. 359-373.

Zienkiewicz, O. C., Taylor, R. L., Zhu J. Z., 2005, *The Finite Element Method: Its Basis & Fundamentals*, 6nd edition, Elsevier, USA.

ACKNOWLEDGEMENT

The authors are grateful to Prof. Krister Svanberg from Royal Institute of Technology, Stockholm, for providing his Matlab version of MMA.